PHYSICAL REVIEW D **80,** 074005 (2009)

Semileptonic decays of the B_c meson

N. Barik,[1,*] Sk. Naimuddin,[2,†] P. C. Dash,[3] and Susmita Kar[4]

[1]*Department of Physics, Utkal University, Bhubaneswar-751004, India*
[2]*Department of Physics, Maharishi College of Natural Law, Bhubaneswar-751007, India*
[3]*Department of Physics, Prananath Autonomous College, Khurda-752057, India*
[4]*Department of Physics, North Orissa University, Baripada-757003, India*

(Received 31 August 2009; published 5 October 2009)

We study the semileptonic transitions $B_c \to \eta_c, J/\Psi, D, D^*, B, B^*, B_s, B_s^*$ in the leading order in the framework of a relativistic independent quark model based on a confining potential in the equally mixed scalar-vector harmonic form. We compute relevant weak form factors as overlap integrals of the meson-wave functions obtained in the relativistic independent quark model in the whole accessible kinematical range. We predict that the semileptonic transitions of the B_c meson are mostly dominated by two Cabibbo-Kobayashi-Maskawa (CKM)-favored modes, $B_c \to B_s(B_s^\star)e\nu$, contributing about 77% of the total decay width, and its decays to vector meson final states take place in the predominantly transverse mode. Our predicted values for the total decay rates, branching ratios, polarization ratios, the forward-backward asymmetry factor, etc., are broadly in agreement with other model predictions.

DOI: 10.1103/PhysRevD.80.074005 PACS numbers: 13.20.He, 12.39.Pn, 13.25.Hw

I. INTRODUCTION

Ever since the discovery of B_c meson by the Collider Detector at Fermilab (CDF) Collaborations [1] in 1998 in the semileptonic decay mode $B_c \to J/\psi + l + \nu_l$, a great deal of attention has been paid to the production mechanism, spectroscopy, and decay properties of B_c meson. The observed values of the B_c-meson mass and lifetime are $M_{B_c} = 6.40 \pm 0.39 \pm 0.13$ GeV and $\tau_{B_c} = 0.46^{+0.18}_{-0.16}(\text{stat}) \pm 0.03(\text{syst})$ ps. Observations of $B_c \to J/\psi + \mu + X$ and its reported preliminary evidence also point towards these values as $M_{B_c} = 5.95^{+0.14}_{-0.13} \pm 0.34$ GeV and $\tau_{B_c} = 0.45^{+0.12}_{-0.10} \pm 0.12$ ps [2]. Much larger samples of B_c mesons and more information on their decay properties are expected from the current run II at Tevatron [3] and the ongoing experiments at the CERN LHC [4]. The dedicated detectors BTeV and LHCB which are especially designed to analyze B physics are expected to provide an essential increase in the statistics up to 10^{10} B_c events per year.

The study of the B_c meson is in fact of great theoretical interest due to its special features. The characteristic feature of the B_c meson is that it is the only quark-antiquark lowest bound-state system composed of heavy quarks ($b\bar{c}$) of different flavors. Both the constituent quarks being heavy, B_c^--meson weak decays can be viewed at the constituent level via (i) b decay, (ii) $\bar{c}$ decay, and also (iii) an annihilation channel providing comparable contributions to the total decay rate. The transitions (i) with spectator $\bar{c}$ induce the semileptonic decays to charmonium and D-meson states, while the transitions (ii) with spectator b induce the semileptonic decays to B_s- and B-meson states. The estimates of the B_c-decay rates indicate that the $\bar{c}$ decay modes provide the dominant 70% contribution while the b decay modes contribute about 20% to the total decay rate. The weak annihilation channels contribute a minimal 10% only [4]. The four-momentum transfer squared "q^2" which provides the kinematic range for the semileptonic B_c^--decay modes varies in wide ranges. It varies from $q^2 = 0$ to $q^2_{\text{max}} \simeq 10$ GeV^2 for the decays to charmonium and from $q^2 = 0$ to $q^2_{\text{max}} \simeq 18$ GeV^2 for decays to D mesons pertaining to transition (i). However, the allowed kinematic range is rather much smaller which is from $q^2 = 0$ to $q^2_{\text{max}} \simeq 1$ GeV^2 only for decays to B and B_s mesons pertaining to transition (ii). As a result, in the B_c-meson rest frame, the maximum recoil momentum of the final charmonium and D mesons is of the same order of magnitude as their masses, while for B_s- and B-meson final states it is considerably smaller than the meson masses. The significant kinematic difference between the b-quark and $\bar{c}$-antiquark decay modes makes it worthwhile to consider the transitions (i) and (ii) separately while investigating the exclusive semileptonic B_c^--meson decays.

B_c-meson decays have been widely studied in the literature after the pioneering paper written by Bjorken in 1986 [5]. In early works based on potential models [6–13], various techniques were used to yield close estimates for the B_c-meson semileptonic decays. Subsequently, these decays were studied in the context of other different models such as the relativistic constituent quark models [14,15], the nonrelativistic constituent quark model [16], the instantaneous nonrelativistic approach to the Bethe-Salpeter equation [17], the three-point sum rules of QCD and nonrelativistic QCD [18], the light cone QCD sum rule [19], application of the heavy quark symmetry (HQS) relation [20,21] to the quark model and the model [22] based on the Isgur, Scora, Grinstein, and Wise wave func-

*nbarik@iopb.res.in
†naim@iopb.res.in

tion, etc. Surprisingly enough, Bjorken's [5] early estimates of the total widths and branching fractions, etc., are found more or less in agreement with the predictions of most of the studies [6–21] made over the years.

The semileptonic decay amplitudes, as usual, find covariant expansion in terms of some weak decay form factors. The relevant form factors can be represented as overlap integrals of the participating hadron wave functions defined in the framework of any suitable model, which then enables one to find the q^2 dependence of the form factors. A reliable analysis of the form factors is, therefore, possible if one can determine their q^2 dependence in the allowed kinematic range. In most of the studies [6–21] cited above, the relevant form factors and their q^2 dependence are, however, determined with an end point normalization at either $q^2 = 0$ or $q^2 = q^2_{\max}$ and then extrapolated to the entire kinematic range using some phenomenological monopole/dipole/Gaussian ansatz. This might have allowed possible uncertainties into these theoretical calculations.

However, the model we would like to adopt here is a relativistic independent quark model (RIQM) [23–25] based on an average confining potential in equally mixed scalar-vector harmonic form. In earlier applications of this model, we have reproduced hadronic static properties [23] like hyperfine mass splitting, an electromagnetic form factor, and charge radii of light mesons and weak leptonic decay constants. We have also described satisfactorily a wide ranging hadronic phenomena including the decays of hadrons [24,25] such as leptonic, weak leptonic, semileptonic, radiative, weak radiative, rare radiative, and radiative leptonic decays, etc. In this paper, we would like to extend the applicability of this model to study both the b-quark and $\bar{c}$-antiquark decay modes of the B_c meson in its semileptonic decays. We would calculate the overlap integrals representing the weak form factors in the framework of the RIQM and determine their q^2 dependence in the entire kinematical range as is done in Ref. [15] without resorting to any kind of phenomenological ansatz for end point normalization, thereby avoiding extrapolation and thus reducing any possible uncertainties in this respect in the calculation.

The paper is organized as follows. In Sec. II we provide the general formalism and the kinematics for B_c-meson semileptonic decays. Section III briefly describes the framework of the underlying RIQM [22–24]. The model expressions for the relevant form factors and their q^2 dependence in the allowed kinematic range are described in Sec. IV. We discuss our numerical results in Sec. V, and finally in Sec. VI, we briefly summarize our results.

II. GENERAL FORMALISM AND KINEMATICS

The invariant transition matrix element for the exclusive semileptonic decays $M \to me\nu$ is written as [26]

$$\mathcal{M} = \frac{G_F}{\sqrt{2}} V_{qq'} l^\mu h_\mu, \tag{1}$$

where G_F is the effective Fermi-coupling constant, $V_{qq'}$ is the Cabibbo-Kobayashi-Maskawa (CKM) parameter, and l^μ and h_μ, respectively, are the leptonic and hadronic amplitudes expressed as

$$l^\mu = \bar{U}_e(\vec{p}_1, \delta_1)\gamma^\mu(1 - \gamma_5)V_\nu(\vec{p}_2, \delta_2), \tag{2}$$

$$h_\mu = \langle m(\vec{k}, S_m)|J^h_\mu(0)|M(\vec{p}, S_M)\rangle. \tag{3}$$

Here $J^h_\mu = V_\mu - A_\mu$ is the vector-axial vector current. We take here (M, m) to be the mass, (p, k) the four momentum, and (S_M, S_m) the spin projection of the parent (M) and daughter (m) meson, respectively. $q = (p - k) = (p_1 + p_2)$ is the four-momentum transfer, and (p_1, p_2) are the four momenta of the lepton pair. We introduce here a pair of dimensionless variables (y, x) scaled to the parent meson mass as $y = (q^2/M^2)$ and $x = (p.p_2/M^2)$ for the sake of convenience to describe the kinematics of the decay process. In the vanishing lepton mass limit, the kinematically allowed range of y is

$$0 \le y \le \left(1 - \frac{m}{M}\right)^2. \tag{4}$$

We also consider two frames of reference: (i) the parent meson rest frame and (ii) the $e\nu$ center-of-mass frame. The coordinate system chosen here is such that the daughter meson momentum $\vec{k}$ is along the negative Z axis with the charged lepton momentum $\vec{p}_1$ subtending an angle θ_e to the Z axis [Fig. 1(a)] in the $e\nu$ center-of-mass frame. The Y axis is oriented perpendicular to the plane containing the final particles' momenta.

In the decay process, the physical quantities of interest associated with the final state particles are their energy and momentum, which can be calculated in both of the frames considered here. In the $e\nu$ center-of-mass frame, they are

$$E_1 = E_2 = \frac{M}{2}\sqrt{y}, \tag{5}$$

$$E_m = \frac{M}{2\sqrt{y}}\left(1 - \frac{m^2}{M^2} - y\right), \tag{6}$$

$$|\vec{k}| = K/\sqrt{y}, \tag{7}$$

$$K = \frac{M}{2}\left[\left(1 - \frac{m^2}{M^2} - y\right)^2 - 4\frac{m^2}{M^2}y\right]^{1/2}. \tag{8}$$

In the parent meson rest frame, however, the quantities are

$$\tilde{E}_1 = Mx = \frac{K}{2}\cos\theta_e + \frac{M}{4}\left(1 - \frac{m^2}{M^2} + y\right), \tag{9}$$

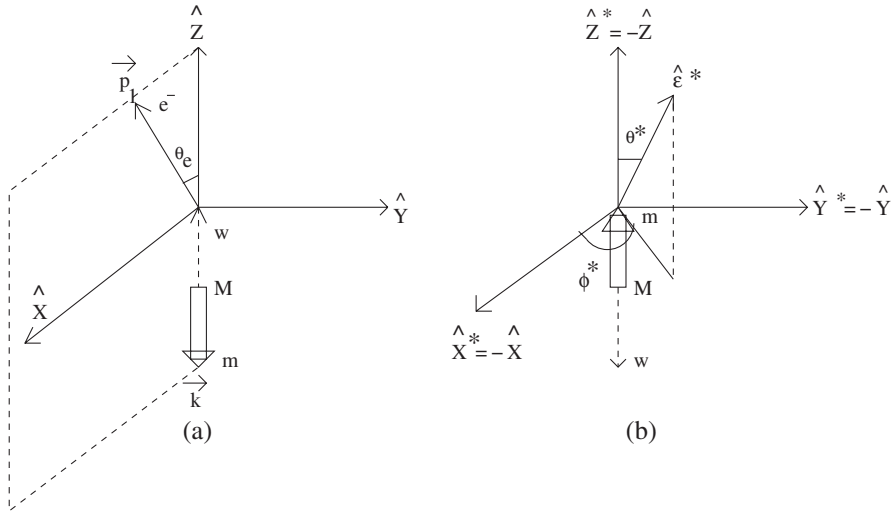

FIG. 1. Coordinate system for the semileptonic decay of meson M. (a) The $e\nu$ center-of-mass frame. (b) The vector meson helicity frame.

$$\tilde{E}_m = \frac{M}{2}\left(1 + \frac{m^2}{M^2} - y\right), \tag{10}$$

$$|\tilde{\vec{k}}| = K. \tag{11}$$

The hadronic amplitudes corresponding to vector and axial vector currents conventionally find covariant expansion in terms of some Lorentz invariant form factors. For $(0^- \to 0^-)$-type transitions these amplitudes are written in the form

$$\langle m(k)|V_\mu(0)|M(p)\rangle = f_+(q^2)(p+k)_\mu + f_-(q^2)(p-k)_\mu, \tag{12}$$

and for $(0^- \to 1^-)$-type transitions these are

$$\langle m(k,\epsilon^*)|V_\mu(0)|M(p)\rangle = ig(q^2) \in_{\mu\nu\rho\sigma} \epsilon^{*\nu}(p+k)^\rho(p-k)^\sigma, \tag{13}$$

$$\langle m(k,\epsilon^*)|A_\mu(0)|M(p)\rangle = f(q^2)\epsilon^*_\mu + a_+(q^2)(\epsilon^*.p)(p+k)_\mu - a_-(q^2)(\epsilon^*.p)(p-k)_\mu. \tag{14}$$

Here $\epsilon^* \equiv (\epsilon^*_0, \vec{\epsilon}^*)$, with $\epsilon^*.k = 0$, represents the vector meson polarization.

The differential decay rate is written in the generic form

$$d\Gamma = \frac{1}{2E_M}\sum_{\delta_1,\delta_2,\lambda} |\mathcal{M}|^2 d\Pi_3, \tag{15}$$

where the three-body phase space factor is

$$d\Pi_3 = (2\pi)^4\delta^{(4)}(p - p_1 - p_2 - k)\frac{d^3\vec{k}}{(2\pi)^3 2E_m}\frac{d^3\vec{p}_1}{(2\pi)^3 2E_1} \times \frac{d^3\vec{p}_2}{(2\pi)^3 2E_2} \tag{16}$$

and the invariant transition amplitude squared is given by

$$\sum_{\delta_1,\delta_2,\lambda} |\mathcal{M}|^2 = \frac{G_F^2}{2}|V_{qq'}|^2 L^{\mu\sigma}H_{\mu\sigma}. \tag{17}$$

We write $L^{\mu\sigma} = \sum_{\delta_1,\delta_2}(l^\mu l^{\sigma\dagger})$ representing a sum over the lepton spin indices (δ_1, δ_2) and also $H_{\mu\sigma} = \sum_\lambda (h_\mu h^\dagger_\sigma)$ representing a sum over the daughter meson (vector) polarization index "λ."

It is often convenient to consider $|\mathcal{M}|^2$ in the $e\nu$ center-of-mass frame in which the timelike part L^{00} of leptonic tensor $L^{\mu\sigma}$ obtained from the trace calculation in the form

$$L^{\mu\sigma} = 8[(p_1^\mu p_2^\sigma - p_1.p_2 g^{\mu\sigma} + p_2^\mu p_1^\sigma) + i\epsilon^{\mu\alpha\sigma\beta}p_{1\alpha}p_{2\beta}] \tag{18}$$

is zero in the vanishing lepton mass limit. With the only nonvanishing spacelike term L^{ij}, the product $L^{\mu\sigma}H_{\mu\sigma}$ in Eq. (17) is reduced to the form $L^{ij}H_{ij}$. Then, integrating the L^{ij} part of $|\mathcal{M}|^2$ over the lepton phase space, one gets in the $e\nu$ center-of-mass frame

$$\iint \frac{d^3\vec{p}_1}{2E_1}\frac{d^3\vec{p}_2}{2E_2}L^{ij}\delta^{(4)}(p - p_1 - p_2 - k) = \frac{4\pi}{3}q^2\delta^{ij}, \tag{19}$$

which reduces the effective hadronic part H_{ij} to H_{ii}. With this consideration, the expression of the differential decay rate (15), in the $e\nu$ center-of-mass frame, is transformed to the form

$$d\Gamma = \frac{1}{(2\pi)^5}\frac{1}{2E_M}\frac{G_F^2}{2}|V_{Qq}|^2\frac{d^3\vec{k}}{2E_m}\frac{4\pi}{3}q^2 H_{ii}. \quad (20)$$

It is worthwhile to note here that the hadronic amplitude "h_i" can be expressed, in this frame, in the simple and convenient form as the terms involving the form factors $f_-(q^2)$ and $a_-(q^2)$ in Eqs. (12) and (14) do not contribute to $\vec{h}$ pertaining to transitions of the type $(0^- \to 0^-)$ and $(0^- \to 1^-)$, respectively. For $(0^- \to 0^-)$-type transitions, one obtains the h_i from Eq. (12) in terms of a single form factor $f_+(q^2)$ as

$$\vec{h} = (\vec{p} + \vec{k})f_+(q^2), \quad (21)$$

Similarly, for transitions of the type $(0^- \to 1^-)$, it is straightforward to find from Eqs. (13) and (14) that

$$\vec{h} = 2i\sqrt{y}Mg(q^2)(\vec{\epsilon}^* \times \vec{k}) - f(q^2)\vec{\epsilon}^* - 2(\epsilon^*.p)a_+(q^2)\vec{k}. \quad (22)$$

For the calculation of physical quantities, it is more convenient to use helicity amplitudes, which are linearly related to the invariant form factors [27]. We, therefore, expand $\vec{h}$ in terms of a helicity basis (effectively of the virtual W) as

$$\vec{h} = \mathcal{H}_+\hat{e}_+ + \mathcal{H}_-\hat{e}_- + \mathcal{H}_0\hat{e}_0, \quad (23)$$

with

$$\hat{e}_\pm = \frac{1}{\sqrt{2}}(\mp\hat{x} - i\hat{y}), \qquad \hat{e}_0 = \hat{z}. \quad (24)$$

The polarization vector $\hat{\epsilon}^*$ with the polar and azimuthal angle (θ^*, ϕ^*) in the vector meson helicity frame [Fig. 1(b)] can be Lorentz-transformed to the $(e\nu)$ center-of-mass frame to be obtained in the form

$$\hat{\epsilon}^* = \frac{1}{\sqrt{2}}\sin\theta^* e^{i\phi^*}\hat{e}_+ - \frac{1}{\sqrt{2}}\sin\theta^* e^{-i\phi^*}\hat{e}_- - \frac{E_m}{m}\cos\theta^*\hat{e}_0. \quad (25)$$

Then expanding h_i in terms of the helicity basis (23) and (24) and using the Lorentz-transformed form of $\hat{\epsilon}^\star$ (25), one can obtain the helicity amplitudes $\mathcal{H}_\pm$ and $\mathcal{H}_0$ from Eq. (22) as

$$\mathcal{H}_\pm = \mp\frac{\sin\theta^*}{\sqrt{2}}e^{\pm i\phi^*}H_\pm, \quad (26)$$

$$\mathcal{H}_0 = \cos\theta^* H_0, \quad (27)$$

where $H_\pm$ and H_0 are reduced helicity amplitudes. For $(0^- \to 1^-)$-type semileptonic transitions, these reduced helicity amplitudes are obtained in terms of the invariant form factors $f(q^2)$, $g(q^2)$, and $a_+(q^2)$ as follows:

$$H_\pm = [f(q^2) \mp 2MKg(q^2)], \quad (28)$$

$$H_0 = \frac{M}{2m\sqrt{y}}\left[\left(1 - \frac{m^2}{M^2} - y\right)f(q^2) + 4K^2 a_+(q^2)\right]. \quad (29)$$

Now $H_{ii} = \sum_\lambda h_i h_i^\dagger$ in Eq. (20) can be expressed in terms of reduced helicity amplitudes (28) and (29), then integrated over the polar and azimuthal angles (θ^*, ϕ^*), and finally summed over the daughter meson (vector) polarization states to yield an invariant expression for the differential decay rate. Once obtained in an invariant form, it is then convenient to cast in any frame (here the parent meson rest frame) so as to get the final expression of the differential decay rate as

$$\frac{d\Gamma}{dy} = \frac{1}{96\pi^3}G_F^2|V_{qq'}|^2M^2Ky[|H_+|^2 + |H_-|^2 + |H_0|^2]. \quad (30)$$

Here the contribution of the $|H_0|^2$ term to the differential decay rate (30) refers to the longitudinal mode, and that of the combined term $[|H_+|^2 + |H_-|^2]$ refers to the transverse polarization mode for the semileptonic transitions of the type $(0^- \to 1^-)$. However, in case of $(0^- \to 0^-)$-type transitions, one can realize the corresponding expressions by appropriately identifying

$$H_\pm = 0, \qquad H_0 = -2\frac{K}{\sqrt{y}}f_+(q^2), \quad (31)$$

which leads to the differential decay rate in parent meson rest frame as

$$\frac{d\Gamma}{dy} = \frac{G_F^2|V_{qq'}|^2K^3M^2}{24\pi^3}|f_+(q^2)|^2. \quad (32)$$

Thus the study of exclusive semileptonic decays such as $M \to me\nu$ is essentially reduced to the evaluation of relevant form factors $f(q^2)$, $g(q^2)$, $a_+(q^2)$, and $f_+(q^2)$ and their q^2 dependence over the allowed kinematic range. We would like to do so by calculating the hadronic matrix elements in the framework of the RIQM described in the following section.

III. TRANSITION MATRIX ELEMENT AND WEAK DECAY FORM FACTORS

The semileptonic decays of the B_c meson composed of two heavy constituents $(b, \bar{c})$ are described at the constituent level via two types of Feynman diagrams [Figs. 2(a) and 2(b)]. Here Fig. 2(a) represents its constituent b-quark decay $[b \to (c, u)W]$ to a less heavy c or a light u quark with the antiquark constituent $\bar{c}$ remaining a mere spectator. In the process, the daughter quark (c, u) and the spectator $\bar{c}$ hadronize to the charmonium $(\eta_c, J/\psi)$ or $(D, D^\star)$ meson states. The emitted W boson ultimately disintegrates to the lepton pair (e, ν_e). The other diagram [Fig. 2(b)] represents its constituent antiquark $\bar{c}$ decay $[\bar{c} \to (\bar{s}, \bar{d})W]$ to the light flavored antiquark ($\bar{s}$ or $\bar{d}$) with the b quark playing the spectator. In the process, the

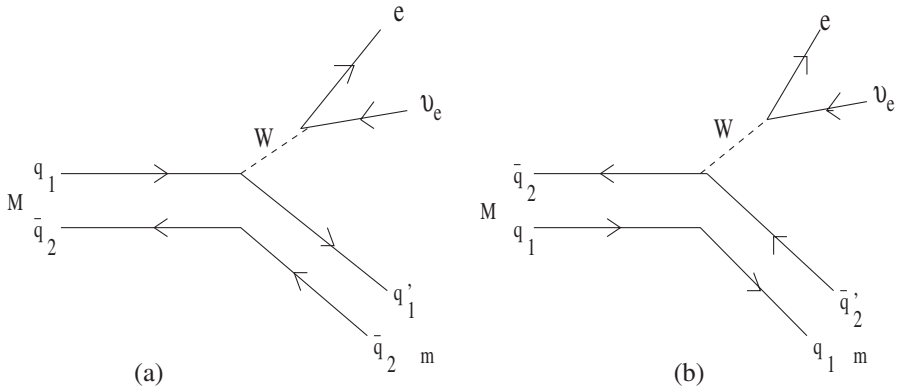

FIG. 2. Semileptonic decay: $M \to me\nu_e$.

daughter ($\bar{s}$ or $\bar{d}$) and spectator b hadronize to (B_s, $B_s^\star$) or (B_d, $B_d^\star$) meson states, and the emitted W boson decays to the lepton pair (e, ν_e). In fact, decay occurs physically between momentum eigenstates of the participating hadrons. Therefore, in a field theoretic calculation of the decay process, the meson state is to be represented by an appropriate momentum wave packet reflecting the momentum and spin distribution between the constituent quark and antiquark inside the meson core. Thus, starting with the basic weak transition at the constituent level, one needs to realize the invariant transition matrix element "$\mathcal{M}$" at the mesonic level on the basis of a suitable constituent quark model.

A. Transition matrix for $M \to me\nu$

The S-matrix element for the semileptonic transition $M \to me\nu$ corresponding to the diagrams depicted in Figs. 2(a) and 2(b) can be written in the general form

$$S_{fi} = i\frac{G_F V_{q_j q'_j}}{\sqrt{2}(2\pi)^4}\int d^4x_1 d^4x_2 d^4q e^{-iq(x_2-x_1)}\langle e(\vec{p}_1,\delta_1) \times \nu(\vec{p}_2,\delta_2) m(\vec{k},S_m)|{:}J_l^\mu(x_2)J_\mu^h(x_1){:}|M(\vec{p},S_M)\rangle, \tag{33}$$

where $q = p - k = p_1 + p_2$ stands for the four-momentum transfer and, with $\Gamma^\mu = \gamma^\mu(1-\gamma_5)$,

$$\begin{aligned} {:}J_l^\mu(x_2){:} &= \bar{\psi}_e^{(-)}(x_2)\Gamma^\mu\psi_\nu^{(-)}(x_2), \\ {:}J_\mu^h(x_1){:} &= \bar{\psi}_{q'_j}^{(-)}(x_1)\Gamma_\mu\psi_{q_j}^{(+)}(x_1). \end{aligned} \tag{34}$$

$|M(\vec{p},S_M)\rangle$ and $|m(\vec{k},S_m)\rangle$ represent the parent and daughter meson state, respectively. In the present model, the momentum wave packet description of the meson corresponding to a definite momentum ($\vec{p}$) and spin (S_M) state is taken in the general form [24,25]

$$|M(\vec{p},S_M)\rangle = \frac{1}{\sqrt{N_M(\vec{p})}}\sum_{\lambda_1,\lambda_2\in S_M}\zeta^M_{q_1,\bar{q}_2}(\lambda_1,\lambda_2)\int d^3\vec{p}_{q_1}d^3\vec{p}_{q_2} \times \delta^{(3)}(\vec{p}_{q_1}+\vec{p}_{q_2}-\vec{p})\mathcal{G}_M(\vec{p}_{q_1},\vec{p}_{q_2}) \times \hat{b}^\dagger_{q_1}(\vec{p}_{q_1},\lambda_1)\hat{\bar{b}}^\dagger_{q_2}(\vec{p}_{q_2},\lambda_2)|0\rangle, \tag{35}$$

where $\hat{b}^\dagger_{q_1}(\vec{p}_{q_1},\lambda_1)$ and $\hat{\bar{b}}^\dagger_{q_2}(\vec{p}_{q_2},\lambda_2)$ are, respectively, the quark and antiquark creation operator. $\zeta^M_{q_1,\bar{q}_2}(\lambda_1,\lambda_2)$ stands for the $SU(6)$-spin flavor coefficients for the meson state. $N_M(\vec{p})$ is the meson normalization realized from $\langle M(\vec{p})|M(\vec{p}')\rangle = \delta^{(3)}(\vec{p}-\vec{p}')$ in the integral form

$$N_M(\vec{p}) = \int d^3\vec{p}_{q_1}|\mathcal{G}_M(\vec{p}_{q_1},\vec{p}-\vec{p}_{q_1})|^2. \tag{36}$$

Finally, $\mathcal{G}_M(\vec{p}_{q_1},\vec{p}-\vec{p}_{q_1})$, which represents the effective momentum distribution function for the quark q_1 and antiquark $\bar{q}_2$, is taken in the form [24,25]

$$\mathcal{G}_M(\vec{p}_{q_1},\vec{p}-\vec{p}_{q_1}) = \sqrt{G_{q_1}(\vec{p}_{q_1})\tilde{G}_{\bar{q}_2}(\vec{p}-\vec{p}_{q_1})}. \tag{37}$$

Here $G_{q_1}(\vec{p}_{q_1})$ and $\tilde{G}_{\bar{q}_2}(\vec{p}-\vec{p}_{q_1})$ refer to the momentum probability amplitude of the bound quark q_1 with momentum $\vec{p}_{q_1}$ and of the antiquark $\bar{q}_2$ with momentum $\vec{p}-\vec{p}_{q_1}$, respectively. The bound quark and antiquark inside the meson core are, in fact, in the definite energy states with no definite momenta of their own. However, it is possible to obtain their momentum probability amplitudes via suitable momentum space projection of the corresponding quark-antiquark eigenmodes derivable from the model. The model expression for $G_{q_1}(\vec{p}_{q_1})$ derived from the eigenmode $\phi^{(+)}_{q_1,\lambda_1}(\vec{r})$ [24,25] is

$$G_{q_1}(\vec{p}_{q_1}) = \frac{i\pi\mathcal{N}_{q_1}}{2\alpha_{q_1}\omega_{q_1}}\left[\frac{\epsilon_{q_1}(\vec{p}_{q_1})}{E_{q_1}(\vec{p}_{q_1})}\right]^{1/2}[E_{q_1}(\vec{p}_{q_1})+E_{q_1}] \times \exp\left(-\frac{\vec{p}^{\,2}_{q_1}}{4\alpha_{q_1}}\right). \tag{38}$$

A similar expression for $\tilde{G}_{\bar{q}_2}(\vec{p}-\vec{p}_{q_1})$ is realized from the

eigenmode $\phi^{(-)}_{q_2,\lambda_2}(\vec{r})$ [24,25] so as to get for like flavors

$$\tilde{G}_{\bar{q}_2}(\vec{p}-\vec{p}_{q_1}) = G^{\star}_{\bar{q}_2}(\vec{p}-\vec{p}_{q_1}). \tag{39}$$

Here $E_{q_j}(\vec{p}_{q_j}) = \sqrt{\vec{p}^2_{q_j} + m^2_{q_j}}$, $\epsilon_{q_j}(\vec{p}_{q_j}) = E_{q_j}(\vec{p}_{q_j}) + m_{q_j}$, and $(\mathcal{N}_q, E_q, \omega_q, \alpha_q)$ are the model quantities as defined in Refs. [24,25].

We may point out here that the bound-state picture of the meson that one can construct in a definite momentum and spin state as in Eq. (35) is not relativistically covariant. This is in fact true with almost all of the potential models describing mesons as bound states of valence quarks and antiquarks interacting via some instantaneous potential. However, such models are often required to derive the mesonic level decay amplitudes starting with the Feynman amplitudes at the constituent quark level. A problem that one usually encounters here is that, although three-momentum conservation at the composite level of the meson has been ensured through $\delta^{(3)}(\vec{p}_{q_1} + \vec{p}_{q_2} - \vec{p})$ in the expression for the meson state $|M(\vec{p}, S_M)\rangle$ in Eq. (35), the energy conservation $E_M = E_{q_1}(\vec{p}_{q_1}) + E_{q_2}(\vec{p}_{q_2})$ in such a definite momentum state cannot be specified so explicitly. This is indeed a pathological problem common to all such models attempting to explain the hadron decays in terms of constituent level dynamics in zeroth order. However, it is quite reassuring to note here that the effective momentum profile function $\mathcal{G}_M(\vec{p}_{q_1}, \vec{p}_{q_2})$, defined through Eqs. (35)–(37) in this model, somehow ensures the energy conservation in an average sense, satisfying $E_M = \langle M(\vec{p}, S_M)|[E_{q_1}(\vec{p}_{q_1}) + E_{q_2}(\vec{p}_{q_2})]|M(\vec{p}, S_M)\rangle$. This has been shown in our earlier work [25] in the case of the meson state: $|B_u(\vec{p}, S_B)\rangle$ and $|B_c(\vec{p}, S_{B_c})\rangle$ in the context of the radiative leptonic decays of the B_u and B_c meson, respectively. Thus, while representing a meson state as an appropriate wave packet of the constituent quark and antiquark, the bound-state character of the meson is thought to be embedded in the dynamical quantity $\mathcal{G}_M(\vec{p}_{q_1}, \vec{p} - \vec{p}_{q_1})$ in Eq. (35).

With this phenomenological picture showing dynamics of the constituent particles inside the bound-state systems of participating mesons, one can derive the decay amplitudes in terms of model quantities.

Now using the usual lepton field expansion, we obtain the matrix element of the leptonic weak current $J^{\mu}_l(x_2)$ in the simple form

$$\langle e(\vec{p}_1, \delta_1)\nu(\vec{p}_2, \delta_2)|J^{\mu}_l(x_2)|0\rangle = \frac{e^{i(p_1+p_2)x_2}}{\sqrt{(2\pi)^6 2E_1 2E_2}} l^{\mu}, \tag{40}$$

where

$$l^{\mu} = \bar{U}_e(\vec{p}_1, \delta_1)\Gamma^{\mu}V_{\nu}(\vec{p}_2, \delta_2). \tag{41}$$

Next using the usual quark field expansion in the hadronic weak current and appropriate momentum wave packets corresponding to the parent and daughter meson states $|M(\vec{p}, S_M)\rangle$ and $|m(\vec{k}, S_m)\rangle$, respectively, the hadronic matrix element is obtained in the form

$$\langle m(\vec{k}, S_m)|J^h_{\mu}(x_1)|M(\vec{p}, S_M)\rangle = \int \frac{d^3\vec{p}_{q_j}\mathcal{G}_M(\vec{p}_{q_j}, \vec{p} - \vec{p}_{q_j})\mathcal{G}_m(\vec{p}_{q_j} + \vec{k} - \vec{p}, \vec{p} - \vec{p}_{q_j})e^{-i(p_{q_j} - p_{q'_j})x_1}}{\sqrt{(2\pi)^6 N_M(\vec{p})N_m(\vec{k})2E_{q_j}(\vec{p}_{q_j})2E_{q'_j}(\vec{p}_{q_j} + \vec{k} - \vec{p})}} \langle S_m|J_{\mu}(0)|S_M\rangle. \tag{42}$$

Here $E_{q_j}(\vec{p}_{q_j})$ and $E_{q'_j}(\vec{p}_{q_j} + \vec{k} - \vec{p})$ stand for the energy of the nonspectator quark or antiquark of the parent and daughter meson, respectively. $\langle S_m|J_{\mu}|S_M\rangle$ represents symbolically the spin matrix elements of the vector-axial vector current. For the transitions involving constituent quark q_1 decay [Fig. 2(a)], it is obtained in the form

$$\begin{aligned}\langle S_m|J_{\mu}(0)|S_M\rangle = &\sum_{\lambda_1,\lambda'_1,\lambda_2} \zeta^{M}_{q_1,q_2}(\lambda_1, \lambda_2)\zeta^{m}_{q'_1,q_2}(\lambda'_1, \lambda_2) \\ &\times [\bar{U}_{q'_1}(\vec{k} + \vec{p}_{q_1} - \vec{p}, \lambda'_1)\gamma_{\mu}(1 - \gamma_5) \\ &\times U_{q_1}(\vec{p}_{q_1}, \lambda_1)].\end{aligned} \tag{43}$$

The hadronic amplitude for the transition involving the antiquark $\bar{q}_2$ decay [Fig. 2(b)] can be obtained in the similar form (4). However, the relevant spin matrix element is obtained here by replacing the free particle spinors as $U_{q_1}(\vec{p}_{q_1}, \lambda_1) \to V_{q'_2}(\vec{k} + \vec{p}_{q_2} - \vec{p}, \lambda'_2)$ and $\bar{U}_{q'_1}(\vec{p}_{q_1} + \vec{k} - \vec{p}, \lambda'_1) \to \bar{V}_{q_2}(\vec{p}_{q_2}, \lambda_2)$.

Here the free particle spinors $U_{q_j}(\vec{p}_{q_j}, \lambda_j)$ and $V_{q_j}(\vec{p}_{q_j}, \lambda_j)$ are taken as

$$\begin{aligned} U_{q_j}(\vec{p}_{q_j}, \lambda_j) &= \sqrt{\epsilon_{q_j}(\vec{p}_{q_j})}\begin{pmatrix} \chi(\lambda) \\ \frac{\vec{\sigma}.\vec{p}_{q_j}}{\epsilon_{q_j}(\vec{p}_{q_j})}\chi(\lambda) \end{pmatrix}, \\ V_{q_j}(\vec{p}_{q_j}, \lambda_j) &= \sqrt{\epsilon_{q_j}(\vec{p}_{q_j})}\begin{pmatrix} \tilde{\chi}(\lambda) \\ \frac{\vec{\sigma}.\vec{p}_{q_j}}{\epsilon_{q_j}(\vec{p}_{q_j})}\tilde{\chi}(\lambda) \end{pmatrix}, \end{aligned} \tag{44}$$

with

$$\chi(\uparrow) = -\tilde{\chi}(\downarrow) = \begin{pmatrix} 1 \\ 0 \end{pmatrix}, \qquad \chi(\downarrow) = \tilde{\chi}(\uparrow) = \begin{pmatrix} 0 \\ 1 \end{pmatrix}.$$

Using the matrix elements of the leptonic and hadronic weak currents as shown in Eqs. (40) and (42), respectively, one would expect to obtain from Eq. (33) the expression of the S-matrix element for the decay process $M \to me\nu$ in the standard form with an appropriate four-momentum δ function at the mesonic level. However, as described

above, starting with the constituent level picture, the realization of the energy-momentum conservation through a four-momentum delta function explicitly at the mesonic level has not been straightforward. This is because of the fact that, although three-momentum conservation is automatically guaranteed at the mesonic level through the wave packet description (35), the same is not so transparent in the case of energy conservation. However, as shown in our earlier work [25], it is possible to ensure the energy conservation here in an average sense through the momentum profile functions $\mathcal{G}_M(\vec{p}_{q_1}, \vec{p}_{q_2})$ and $\mathcal{G}_m(\vec{p}_{q'_{1(2)}}, \vec{p}_{q_{2(1)}})$ in the parent and daughter meson state, respectively. Taking into account the energy conservation constraints $E_M = E_{q_1}(\vec{p}_{q_1}) + E_{q_2}(\vec{p} - \vec{p}_{q_1})$ and $E_m(\vec{k}) = E_{q'_{1(2)}}(\vec{p}_{q_{1(2)}} + \vec{k} - \vec{p}) + E_{q_{2(1)}}(\vec{p} - \vec{p}_{q_{1(2)}})$ along with the three-momentum conservation $\vec{p} = \vec{p}_{q_1} + \vec{p}_{q_2}$ and $\vec{k} = \vec{p}_{q'_{1(2)}} + \vec{p}_{q_{2(1)}}$ ensured by an appropriate three-momenta delta function in the meson wave packets, we write $p = p_{q_1} + p_{q_2}$ and $k = p_{q'_{1(2)}} + p_{q_{2(1)}}$. Then it is possible to pull out $\delta^{(4)}(p_{q_{1(2)}} - p_{q'_{1(2)}} - p_1 - p_2)$ from the quark level integral of S_{fi} in the form $\delta^{(4)}(p - k - p_1 - p_2)$ which ensures the required four-momentum conservation in the decay process. Then one can write

$$S_{fi} = (2\pi)^4 \delta^{(4)}(p - k - p_1 - p_2)(-i\mathcal{M}_{fi}) \times \frac{1}{\sqrt{(2\pi)^3 2E_M}} \prod_f \left(\frac{1}{\sqrt{(2\pi)^3 2E_f}} \right). \tag{45}$$

We may point out here that the meson normalization factor $1/\sqrt{2E_M 2E_m}$ does not appear automatically in the kinematic expression of S_{fi}. In order to cast it in the standard form, we include this factor by adequately compensating the same in the numerator. The compensating factor $\sqrt{2E_M 2E_m}$ is then pushed inside the quark level integral as

$$\sqrt{2[E_{q_1}(\vec{p}_{q_j}) + E_{q_2}(\vec{p} - \vec{p}_{q_j})]2[E_{q'_{1(2)}}(\vec{p}_{q_j} + \vec{k} - \vec{p}) + E_{q_{2(1)}}(\vec{p} - \vec{p}_{q_j})]} = 2R(\vec{p}_{q_j})$$

under the same assumption with which it was pulled out of the integral as described above. With this, the S-matrix element is realized in the standard form from which the invariant transition amplitude $\mathcal{M}_{fi}$ is extracted as

$$\mathcal{M}_{fi} = \frac{G_F}{\sqrt{2}} V_{q_j q'_j} l^\mu h_\mu, \tag{46}$$

where the invariant hadronic amplitude h_μ is finally obtained in the form

$$h_\mu = \frac{1}{\sqrt{N_M(\vec{p}) N_m(\vec{k})}} \int d^3\vec{p}_{q_j} \frac{R(\vec{p}_{q_j})}{\sqrt{E_{q_j}(\vec{p}_{q_j}) E_{q'_j}(\vec{p}_{q_j} + \vec{k} - \vec{p})}} \times \mathcal{G}_M(\vec{p}_{q_j}, \vec{p} - \vec{p}_{q_j}) \mathcal{G}_m(\vec{p}_{q_j} + \vec{k} - \vec{p}, \vec{p} - \vec{p}_{q_j}) \times \langle S_m | J_\mu(0) | S_M \rangle. \tag{47}$$

B. Weak decay form factors

As discussed earlier in Sec. II, the hadronic amplitudes for the decay process find covariant expansion in terms of the weak form factors (12)–(14) in terms of which the decay rate and polarization fractions, etc., have been expressed as shown in Eqs. (30)–(32). The form factors, being Lorentz invariant quantities, can be calculated in any suitable frame. For the sake of convenience, we choose here the parent meson rest frame for the same. We compare the model expressions for hadronic amplitudes with corresponding expressions from the covariant expansion in Eqs. (12)–(14) in the parent meson rest frame so as to obtain the weak decay form factors in the following manner.

First we calculate the spin matrix elements from Eq. (43) using usual spin algebra. For the $(0^- \to 0^-)$ transitions where only vector current contributes, we get

$$\langle S_m(\vec{k}) | V_0 | S_M(0) \rangle = \frac{[\epsilon_{q'_j}(\vec{p}_{q_j} + \vec{k}) \epsilon_{q_j}(\vec{p}_{q_j}) + \vec{p}^2_{q_j}]}{\sqrt{\epsilon_{q'_j}(\vec{p}_{q_j} + \vec{k}) \epsilon_{q_j}(\vec{p}_{q_j})}}, \tag{48}$$

$$\langle S_m(\vec{k}) | V_i | S_M(0) \rangle = \frac{\epsilon_{q_j}(\vec{p}_{q_j})}{\sqrt{\epsilon_{q'_j}(\vec{p}_{q_j} + \vec{k}) \epsilon_{q_j}(\vec{p}_{q_j})}} k_i. \tag{49}$$

Here, for the sake of brevity, we also write $\epsilon_{q_j}(\vec{p}_{q_j}) = E_{q_j}(\vec{p}_{q_j}) + m_{q_j}$ and $\epsilon_{q'_j}(\vec{p}_{q_j} + \vec{k}) = E_{q'_j}(\vec{p}_{q_j} + \vec{k}) + m_{q'_j}$.

Now substituting the results of Eqs. (48) and (49) in Eq. (47) in the parent meson rest frame and then comparing with the corresponding expressions from Eq. (12), we get the relevant form factor $f_+(q^2)$ for the $(0^- \to 0^-)$-type transition in the form

$$f_+(q^2) = \frac{1}{2M} \int d\vec{p}_{q_j} \mathcal{C}(\vec{p}_{q_j}) [\epsilon_{q_j}(\vec{p}_{q_j}) \{\epsilon_{q'_j}(\vec{p}_{q_j} + \vec{k}) + M - \tilde{E}_m\} + \vec{p}^2_{q_j}], \tag{50}$$

where

$$\mathcal{C}(\vec{p}_{q_j}) = \frac{\mathcal{G}_M(\vec{p}_{q_j}, -\vec{p}_{q_j})\mathcal{G}_m(\vec{p}_{q_j}+\vec{k}, -\vec{p}_{q_j})\sqrt{[E_{q_j}(\vec{p}_{q_j})+E_{q_j}][E_{q'_j}(\vec{p}_{q_j}+\vec{k})+E_{q'_j}]}}{\sqrt{N_M(0)N_m(\vec{k})E_{q_j}(\vec{p}_{q_j})E_{q'_j}(\vec{p}_{q_j}+\vec{k})\epsilon_{q_j}(\vec{p}_{q_j})\epsilon_{q'_j}(\vec{p}_{q_j}+\vec{k})}}. \tag{51}$$

However, for the $(0^- \to 1^-)$-type transitions where both the vector and axial vector currents contribute, the spin matrix elements are obtained separately in the form

$$\langle S_m(\vec{k}, \hat{\epsilon}^*)|V_0|S_M(0)\rangle = 0, \tag{52}$$

$$\langle S_m(\vec{k}, \hat{\epsilon}^*)|V_i|S_M(0)\rangle = \frac{i\epsilon_{q_j}(\vec{p}_{q_j})}{\sqrt{\epsilon_{q_j}(\vec{p}_{q_j})\epsilon_{q'_j}(\vec{p}_{q_j}+\vec{k})}}(\hat{\epsilon}^* \times \vec{k})_i, \tag{53}$$

$$\langle S_m(\vec{k}, \hat{\epsilon}^*)|A_0|S_M(0)\rangle = -\frac{\epsilon_{q_j}(\vec{p}_{q_j})}{\sqrt{\epsilon_{q_j}(\vec{p}_{q_j})\epsilon_{q'_j}(\vec{p}_{q_j}+\vec{k})}}(\hat{\epsilon}^*.\vec{k}), \tag{54}$$

$$\langle S_m(\vec{k}, \hat{\epsilon}^*)|A_i|S_M(0)\rangle = \frac{[\epsilon_{q_j}(\vec{p}_{q_j})\epsilon_{q'_j}(\vec{p}_{q_j}+\vec{k}) - \vec{p}^2_{q_j}/3]}{\sqrt{\epsilon_{q_j}(\vec{p}_{q_j})\epsilon_{q'_j}(\vec{p}_{q_j}+\vec{k})}}\epsilon^*_i. \tag{55}$$

A term by term comparison of the results in Eqs. (53) and (55) with the corresponding expressions obtained from the form factor expansions in Eqs. (13) and (14) gives the relevant form factors "$g(q^2)$" and "$f(q^2)$" in the form

$$g(q^2) = -\frac{\mathcal{A}}{2M} = -\frac{1}{2M}\int d\vec{p}_{q_j}\mathcal{C}(\vec{p}_{q_j})\epsilon_{q_j}(\vec{p}_{q_j}), \tag{56}$$

$$f(q^2) = -\int d\vec{p}_{q_j}\mathcal{C}(\vec{p}_{q_j})[\epsilon_{q_j}(\vec{p}_{q_j})\epsilon_{q'_j}(\vec{p}_{q_j}+\vec{k}) - \vec{p}^2_{q_j}/3]. \tag{57}$$

In the present model we also get $a_+(q^2) = a_-(q^2)$.

Now, in order to find the model expressions of the form factor "$a_+(q^2)$," we calculate the timelike part of the hadronic amplitude (47) due to the axial vector current corresponding to the longitudinal spin polarization of the daughter meson $m(\vec{k}, \hat{\epsilon}^*)$. From the amplitude $\langle m(\vec{k}, \hat{\epsilon}^{*L})|A_0|M(\vec{p}=0)\rangle$ and equality condition $a_+(q^2) = a_-(q^2)$, we get

$$[f(q^2) + 2M^2 a_+(q^2)]\epsilon^{*L}_0 = -\mathcal{A}|\vec{k}|. \tag{58}$$

Note that the spin quantization axis is taken here opposite to the boost direction. As a result, the longitudinal polarization vector $\epsilon^{*(L)}_\mu$ is boosted yielding the timelike component $\epsilon^{*(L)}_0 = -\frac{|\vec{k}|}{m}$ with $\epsilon^{*(T)}_0 = 0$. By substituting this and $\mathcal{A} = -2Mg(q^2)$ (56) in Eq. (58), it is straightforward to find

$$a_+(q^2) = -\frac{1}{2M^2}[f(q^2) + 2Mmg(q^2)]. \tag{59}$$

The model expressions for the form factors $f_+(q^2)$, $g(q^2)$, $f(q^2)$, and $a_+(q^2)$ in Eqs. (50), (56), (57), and (59) are believed to embody their q^2 dependence in the allowed kinematic range. These form factors can also be expressed in the dimensionless form as cited in the literature to treat them on equal footing as

$$\begin{aligned} F_1(q^2) &= f_+(q^2), \\ V(q^2) &= (M+m)g(q^2), \\ A_1(q^2) &= (M+m)^{-1}f(q^2), \\ A_2(q^2) &= -(M+m)a_+(q^2). \end{aligned} \tag{60}$$

With the relevant weak decay form factors expressed in the general form (50), (56), (57), and (59) in terms of the model quantities, it is straightforward to study their q^2 dependence and to evaluate numerically the decay rates and branching ratios for different semileptonic B_c decays using Eqs. (30) and (32). This is done in the following section by appropriate replacement of the flavor degrees of freedom and other related quantities relevant for specific decay modes.

IV. NUMERICAL RESULTS AND DISCUSSION

We must point out at the outset that, for the numerical calculation in the model adopted here, we use the model parameters and model quantities obtained earlier in its applications to several hadronic phenomena in the light as well as heavy flavor sectors [23–25]. Hence we take the constituent quark masses "m_q," corresponding binding energies "E_q," and flavor independent potential parameters (a, V_0) as follows:

$$\begin{aligned} &(m_u = m_d, m_s, m_c, m_b) \\ &\quad \equiv (0.078\,75, 0.315\,75, 1.492\,76, 4.776\,59)\ \text{GeV}, \\ &(E_u = E_d, E_s, E_c, E_b) \\ &\quad \equiv (0.471\,25, 0.591\,00, 1.579\,51, 4.766\,33)\ \text{GeV}, \\ &(a, V_0) \equiv (0.017\,166\ \text{GeV}^3, -0.1375\ \text{GeV}). \end{aligned} \tag{61}$$

For related CKM parameters and B_c meson lifetime, we take their central values from the Particle Data Group [28] as

$$\begin{aligned} (V_{bc}, V_{bu}) &\equiv (0.0412, 0.003\,93), \\ (V_{cs}, V_{cd}) &\equiv (1.04, 0.23), \qquad \tau_{B_c} \equiv 0.46\ \text{ps}. \end{aligned} \tag{62}$$

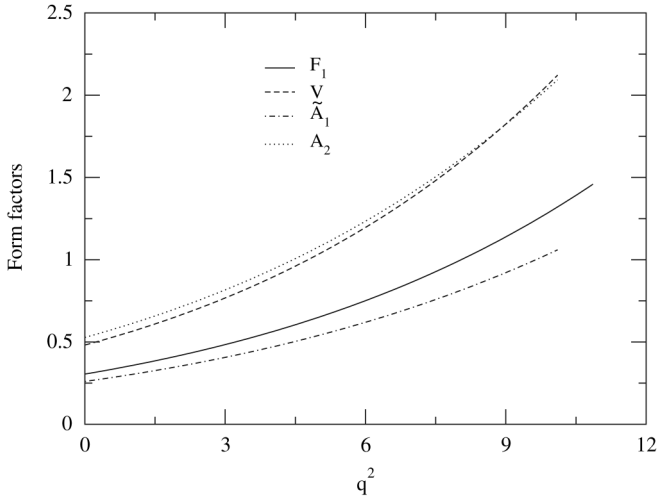

FIG. 3. Form factors of $B_c \to \eta_c, J/\Psi$.

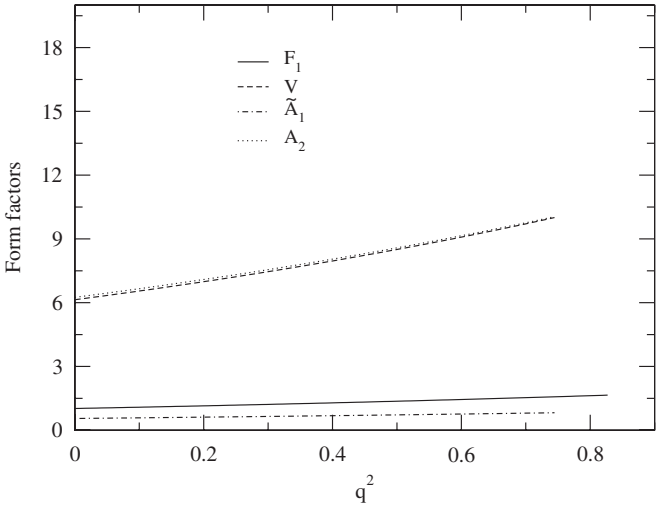

FIG. 5. Form factors of $B_c \to B_s, B_s^*$.

The physical mass of the participating mesons are taken according to the recorded values from Ref. [28] as

$$\begin{aligned} M_{B_c} &= 6.276 \text{ GeV}, \\ (M_{\eta_c}, M_{J/\psi}) &\equiv (2.9803, 3.096\,916) \text{ GeV}, \\ (M_{D^0}, M_{D^{*0}}) &\equiv (1.864\,84, 2.007) \text{ GeV}, \\ (M_{B_s^0}, M_{B_s^{*0}}) &\equiv (5.3666, 5.4131) \text{ GeV}, \\ (M_{B^0}, M_{B^{*0}}) &\equiv (5.2795, 5.325) \text{ GeV}. \end{aligned} \tag{63}$$

With these inputs, we first calculate the weak form factors $f_+(q^2)$, $g(q^2)$, $f(q^2)$, and $a_+(q^2)$ using Eqs. (50), (56), (57), and (59), respectively, from which the q^2 dependence of the equivalent dimensionless form factors F_1, V, A_1, and A_2 are studied in the allowed kinematical range. Our results for the CKM-enhanced: $B_c \to \eta_c(J/\Psi)$ and $B_c \to B_s(B_s^*)$—as well as the CKM-suppressed: $B_c \to D(D^*)$ and $B_c \to B(B^*)$—transitions are depicted in Figs. 3–6. The different behavior (rate of growing with q^2) of the form factors here is attributed to the properties of the final meson-wave functions and the momentum transfer involved in the decay processes. One may naively expect these form factors to satisfy the HQS relations as an outcome of the heavy quark effective theory

$$F_1(q^2) \simeq V(q^2) \simeq A_2(q^2) \simeq \tilde{A}_1(q^2), \tag{64}$$

where

$$\tilde{A}_1(q^2) = \left[1 - \frac{q^2}{(M+m)^2}\right]^{-1} A_1(q^2).$$

Our predictions, however, indicate that all of the form factors do not simultaneously satisfy the HQS relation (64). Only $V(q^2)$ and $A_2(q^2)$ somehow show equality (64) in the allowed physical region, whereas $\tilde{A}_1(q^2)$ and $F_1(q^2)$ do not. This corroborates the well known fact that

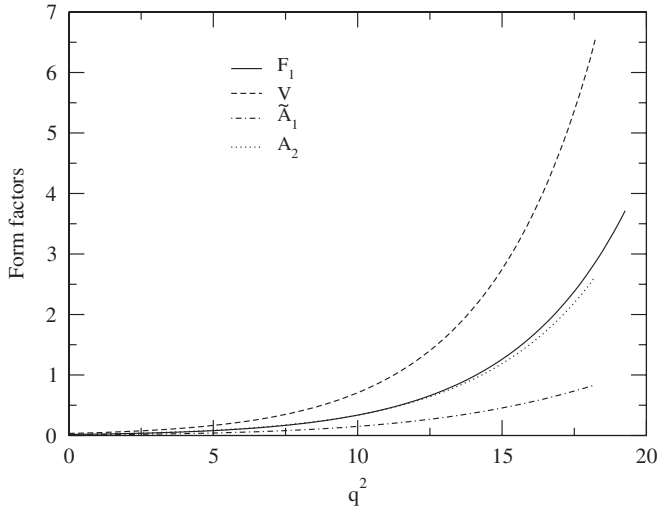

FIG. 4. Form factors of $B_c \to D, D^*$.

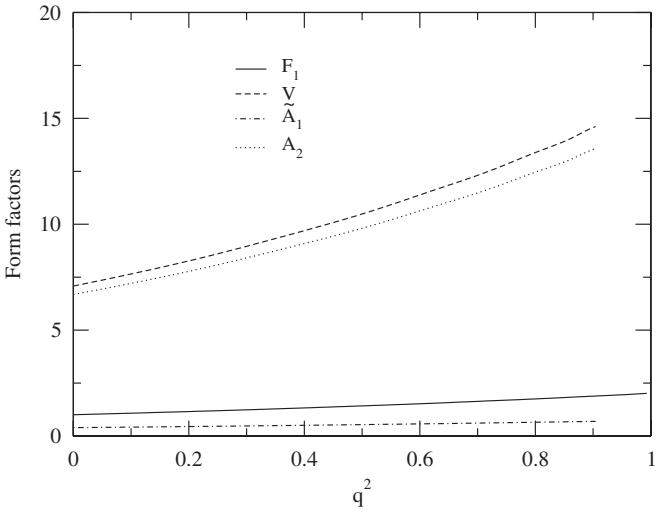

FIG. 6. Form factors of $B_c \to B, B^*$.

TABLE I. Predicted values of the form factors of weak B_c decays.

Transition	$F_1(q^2)$	$V(q^2)$	$A_1(q^2)$	$A_2(q^2)$
$B_c \to \eta_c(J/\Psi)$				
$q^2 = 0$	0.304	0.481	0.260	0.527
$q^2 = q^2_{\max}$	1.459	2.121	0.938	2.093
$B_C \to D(D^*)$				
$q^2 = 0$	0.017	0.034	0.009	0.019
$q^2 = q^2_{\max}$	3.715	6.541	0.615	2.627
$B_c \to B_s(B_s^*)$				
$q^2 = 0$	0.021	6.138	0.552	6.251
$q^2 = q^2_{\max}$	1.649	10.003	0.818	10.046
$B_c \to B(B^*)$				
$q^2 = 0$	1.005	7.082	0.393	6.681
$q^2 = q^2_{\max}$	2.014	14.614	0.688	13.574

the heavy flavor symmetry cannot be strictly used for hadrons containing two heavy quarks [14,27]. Since in $\bar{c} \to \bar{s}, \bar{d}$ induced transitions the momentum transfer is marginal, the effect on the q^2 dependence is rather mild as shown in their near flat behavior. The sizable effect on q^2 dependence of the form factors related to $B_c \to \eta_c(J/\Psi)$ and $B_c \to D(D^*)$ semileptonic decay modes as shown in the rising slope of the curve is due to significant momentum transfer involved in the decay processes. As expected, the effect is most pronounced in the case of $B_c \to D(D^*)$ semileptonic decay modes as the recoil momentum of the final charmed meson states is highest among all of the channels considered here. Our predicted values of the form factors at the maximum and zero recoil point for both the $b \to c, u$ and $\bar{c} \to \bar{s}, \bar{d}$ induced B_c transitions are listed in Table I which are comparable to those of Ref. [15].

The differential decay rates $\frac{d\Gamma}{dq^2}$ for semileptonic B_c decay modes, calculated in the present model using

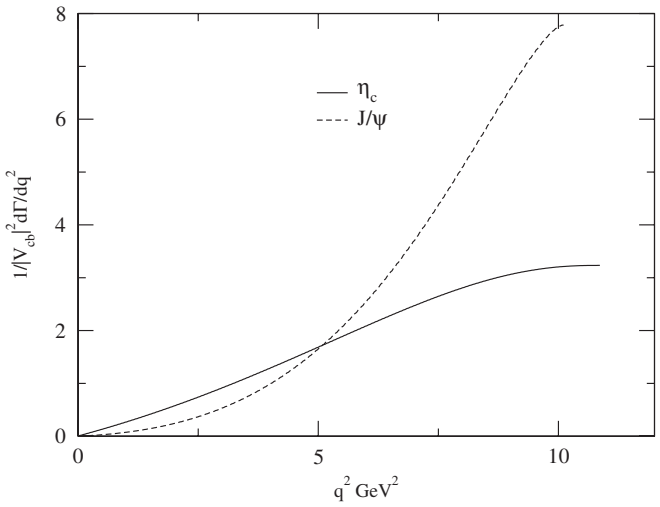

FIG. 7. Differential decay rate of $B_c \to \eta_c(J/\Psi)$ in 10^{-12} GeV.

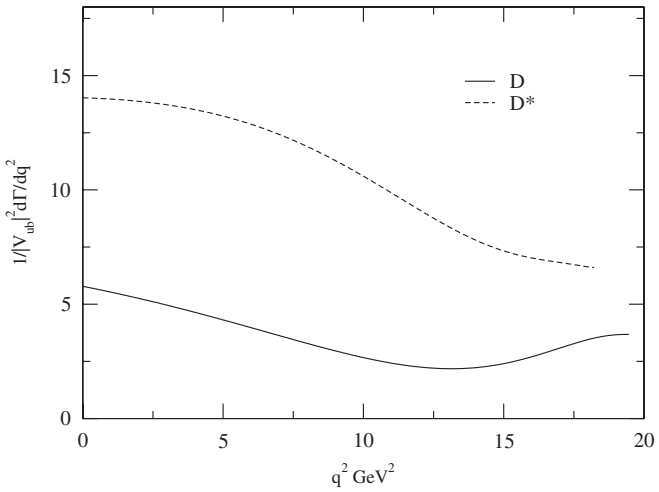

FIG. 8. Differential decay rate of $B_c \to D(D^*)$ in 10^{-12} GeV.

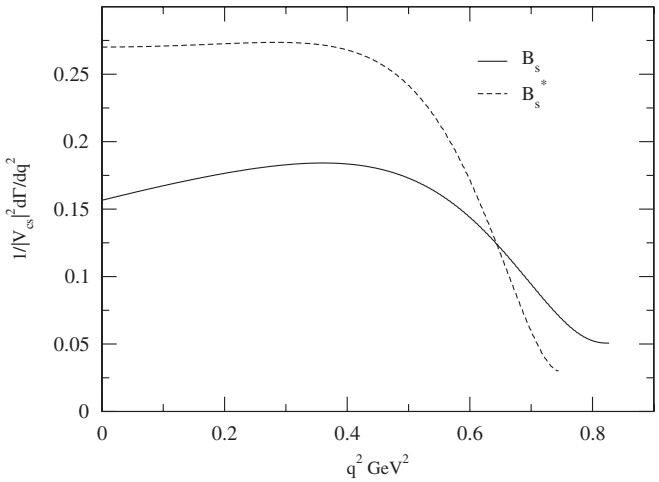

FIG. 9. Differential decay rate of $B_c \to B_s(B_s^*)$ in 10^{-12} GeV.

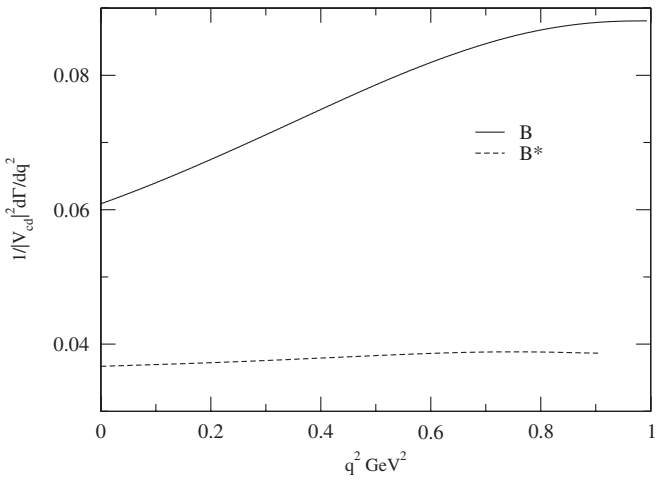

FIG. 10. Differential decay rate of $B_c \to B(B^*)$ in 10^{-12} GeV.

TABLE II. Predicted semileptonic B_c-decay rates "Γ" (in 10^{-15} GeV) and branching ratios "Br" in comparison with other model predictions.

Quark level	Composite level	Γ	Γ	Γ	Γ	Γ	Γ	Γ	Γ	Γ	Γ	Γ	Γ	Predicted
Transition	Transition	[8]	[9]	[10]	[12]	[13]	[14]	[15]	[16]	[18]	[20]	[21]	Our result	Br (in %)
$b \to c$	$B_c^- \to \eta_c e^- \nu$	11.1	14.2	6.8	8.6	8.31	10.70	5.9	6.95	11	8.31	2.1	5.49	0.383
	$B_c^- \to J/\Psi e^- \nu$	30.2	34.4	19.4	17.2	20.3	30.28	17.7	21.9	28	20.3	21.6	13.21	0.923
$b \to u$	$B_c^- \to D^0 e^- \nu$	0.049	0.094	⋯	⋯	0.085	0.051	0.019	⋯	0.059	0.085	0.005	0.057	0.004
	$B_c^- \to D^{*0} e^- \nu$	0.192	0.269	⋯	⋯	0.204	0.055	0.11	⋯	0.27	0.204	0.12	0.103	0.007
$\bar{c} \to \bar{s}$	$B_c^- \to B_s^0 e^- \nu$	14.3	26.6	12.3	15	26.8	16.09	12	⋯	59	11.75	11.1	54.81	3.830
	$B_c^- \to B_s^{*0} e^- \nu$	50.4	44.0	19.0	34	34.6	34.66	25	⋯	65	32.56	33.5	32.68	2.283
$\bar{c} \to \bar{d}$	$B_c^- \to B^0 e^- \nu$	1.14	2.30	⋯	⋯	1.90	1.03	0.6	⋯	4.9	0.59	0.90	4.66	0.326
	$B_c^- \to B^{*0} e^- \nu$	3.53	3.32	⋯	⋯	2.34	0.921	1.7	⋯	8.5	2.44	2.8	2.04	0.143

Eqs. (30) and (32), are plotted in the allowed physical range. The results are shown in Figs. 7–10. We calculate the total decay rates and branching ratios by integrating the corresponding differential decay rates over the allowed q^2 range. Our results are reported in Table II in comparison with the predictions of other approaches based on quark models [8–10,12–16], QCD sum rules [18], and the application of the HQS relation [20,21] to the quark model. In analyzing our results (Table II) for the $b \to c, u$ induced transitions, we find that our predicted values for the CKM-favored decays to the charmonium ground states are almost 2 times smaller than those of the QCD sum rule [18] and quark models [8,9] but comparable those of Refs. [10,12,13,15,20,21]. The ratio of $B_c \to J/\psi e\nu$ to $B_c \to \eta_c e\nu$ decay rates is found close to most of predictions in the literature.

Note that a peculiar role is played by the $B_c \to J/\psi e\nu$ mode due to the possible clear signature represented by three charged leptons from the same decay vertex, two of them coming from J/ψ. This signature has been exploited to identify the B_c meson at the Tevatron [1] and will be mainly employed at the future colliders [21,29]. We predict that the decay width $\Gamma(B_c \to J/\psi e\nu) = 13.21 \times 10^{-15}$ GeV with an upper bound of 13.47×10^{-15} GeV. For the CKM-suppressed modes $B_c \to D(D^*)e\nu$, our results more or less agree with those of Refs. [15,18,21]. Similarly analyzing our results for the $\bar{c} \to \bar{s}, \bar{d}$ induced transitions, we find that our predictions for the CKM-favored $B_c \to B_s^* e\nu$ modes are suppressed compared to those of Refs. [8,9,18] but are in agreement with quark model results [13,14,20,21]. However, for CKM-suppressed $B_c \to B^* e\nu$ modes, our predictions more or less agree with that of Refs. [13,15] and the ones based on the application of the HQS relation [20,21] to the quark model.

TABLE III. Predicted values of the semileptonic B_c decay rates $\Gamma_{L,T,+,-}$ (in 10^{-15} GeV), polarization ratios α, and forward-backward asymmetry $A_{\rm FB}$.

Transition	Γ_L	Γ_T	α	Γ_+	Γ_-	$A_{\rm FB}$
$B_c^- \to J/\Psi e^- \nu$	4.276	8.931	−0.0424	1.678	7.253	0.316
$B_c^- \to D^{*0} e^- \nu$	0.010	0.093	−0.783	0.004	0.089	0.624
$B_c^- \to B_s^{*0} e^- \nu$	7.350	25.326	−0.419	2.629	22.697	0.461
$B_c^- \to B^{*0} e^- \nu$	0.192	1.853	−0.793	0.042	1.811	0.649

From our predictions shown in Table II, we conclude that the semileptonic B_c transitions are mostly dominated by two CKM-favored modes $B_c \to B_s(B_s^*)e\nu$, contributing about 77% of the total decay width, in spite of the small phase space available for the decay processes. The other two CKM-favored channels $B_c \to \eta_c(J/\psi)e\nu$ contribute about 17%, and the remaining four CKM-suppressed semileptonic decay modes contribute hardly 6% of the total width. For the sake of completeness, we also predict separately the longitudinal and transverse polarization states with helicity $\lambda = \pm 1$, the polarization ratio $\alpha = \frac{2\Gamma_0}{\Gamma_+ \Gamma_-} - 1$, and the forward-backward asymmetry factor $A_{\rm FB} = \frac{3}{4} \times (\frac{\Gamma_- - \Gamma_+}{\Gamma})$. Our results shown in Table III indicate that the semileptonic B_c transitions to vector meson final states take place in the predominantly transverse mode in agreement with the quark model predictions [15].

V. SUMMARY AND CONCLUSION

In this paper, we considered the weak semileptonic B_c decays to η_c, J/Ψ; D, D^* and B_s, B_s^*; B B^* meson ground states associated with $b \to c, u$ and $\bar{c} \to \bar{s}, \bar{d}$ quark transitions, respectively, in the framework of the relativistic independent quark model based on the confining potential in equally mixed scalar-vector harmonic form. The weak decay form factors taken as overlap integrals of the meson-wave functions derived from present model dynamics were calculated explicitly in the whole kinematic range. The B_c decay widths, branching ratios, longitudinal and horizontal polarization, and the polarization ratios, etc., were predicted in general agreement with other model predictions. From the results shown in Table II, it is concluded that the semileptonic B_c decays pertaining to transitions of type (i) and (ii) are mostly dominated by two CKM-enhanced $\bar{c} \to \bar{s}$ induced transitions $B_c \to B_s e\nu$ and $B_c \to B_s^* e\nu$, respectively, representing nearly 77% of the total width. The

CKM-favored $b \to c$ induced transitions $B_c \to \eta_c e\nu$ and $B_c \to J/\Psi e\nu$ contribute about 17%, and the remaining four CKM-suppressed channels considered here contribute hardly 6% of the total width. It is also observed that the semileptonic B_c decays to vector $(J/\Psi, D^*, B_s^*, B^*)$ meson ground states are mediated in predominantly transverse mode, as in other quark model calculations, yielding to the predicted values of the polarization ratio "α" and forward-backward asymmetry factor "$A_{\rm FB}$" as reported here. Besides giving new hints to analyze other decay processes such as the flavor changing radiative, nonleptonic, and CP-violating B_c decays, our predictions in this sector can be useful to identify the B_c channels characterized by a clear experimental signature, a large branching ratio, and a visible CP asymmetry in the future accelerator experiments. With possible reliable data on the B_c-decay rates expected from the ongoing experiments at the LHC, one can extract the CKM parameters $V_{q_j q_j'}$ that would represent an important consistency check of the standard model.

[1] F. Abe *et al.* (CDF Collaboration), Phys. Rev. D **58**, 112004 (1998); Phys. Rev. Lett. **81**, 2432 (1998).
[2] M. D. Corcoran (CDF Collaboration and D0 Collaboration), arXiv:hep-ex/0506061.
[3] K. Anikeev *et al.*, arXiv:hep-ph/0201071.
[4] I. P. Gouz *et al.*, Yad. Fiz. **67**, 1581 (2004) [Phys. At. Nucl. **67**, 1559 (2004)].
[5] J. D. Bjorken, report (unpublished).
[6] M. Lusignoli and M. Masetti, Z. Phys. C **51**, 549 (1991).
[7] V. V. Kiselev, Mod. Phys. Lett. A **10**, 1049 (1995); Int. J. Mod. Phys. A **9**, 4987 (1994); V. V. Kiselev, A. K. Likhoded, and A. V. Tkabladze, Phys. At. Nucl. **56**, 643 (1993); Yad. Fiz. **56**, 128 (1993); V. V. Kiselev and A. V. Tkabladze, Yad. Fiz. **48**, 536 (1988); S. S. Gershtein *et al.*, Yad. Fiz. **48**, 515 (1988); G. R. Jibuti and Sh. M. Esakia, Yad. Fiz. **50**, 1065 (1989); **51**, 1681 (1990).
[8] A. Abd El-Hady, J. H. Munoz, and J. P. Vary, Phys. Rev. D **62**, 014019 (2000).
[9] C. H. Chang and Y. Q. Chen, Phys. Rev. D **49**, 3399 (1994).
[10] M. A. Nobes and R. M. Woloshyn, J. Phys. G **26**, 1079 (2000).
[11] D. Scora and N. Isgur, Phys. Rev. D **52**, 2783 (1995).
[12] A. Yu. Anisimov, I. M. Narodetskil, C. Semay, and B. Silvestre-Brac, Phys. Lett. B **452**, 129 (1999); A. Y. Anisimov, P. Yu. Kulikov, I. M. Narodetsky, and K. A. Ter-Martirosyan, Yad. Fiz. **62**, 1868 (1999) [Phys. At. Nucl. **62**, 1739 (1999)].
[13] J. F. Liu and K. T. Chao, Phys. Rev. D **56**, 4133 (1997).
[14] Mikhail A. Ivanov, Juergen G. Korner, and Pietro. Santorelli, Phys. Rev. D **63**, 074010 (2001); **71**, 094006 (2005); **73**, 054024 (2006).
[15] D. Ebert, R. N. Faustov, and V. O. Galkin, Phys. Rev. D **68**, 094020 (2003); Eur. Phys. J. C **32**, 29 (2003).
[16] E. Hernandez, J. Nieves, and J. M. Verde-Velasco, Phys. Rev. D **74**, 074008 (2006); Eur. Phys. J. A **31**, 714 (2007).
[17] C. H. Chang, Y. Q. Chen, G. L. Wang, and H. S. Zong, Phys. Rev. D **65**, 014017 (2001); Commun. Theor. Phys. **35**, 395 (2001).
[18] V. V. Kiselev, A. K. Likhoded, and A. I. Onishchenko, Nucl. Phys. **B569**, 473 (2000); V. V. Kiselev, A. E. Kovalsky, and A. K. Likhoded, Nucl. Phys. **B585**, 353 (2000); V. V. Kiselev, arXiv:hep-ph/0211021.
[19] Tao Huang, Zuo-Hong Li, Xing-Garg Wu, and Fen Zuo, arXiv:0801.0473v2.
[20] G. Lu, Y. Yang, and H. Li, Phys. Lett. B **341**, 391 (1995).
[21] P. Colangelo and F. DeFazio, Phys. Rev. D **61**, 034012 (2000).
[22] G. L. Castro, H. B. Mayorga, and J. H. Munoz, J. Phys. G **28**, 2241 (2002); N. Isgur, D. Scora, B. Grinstein, and M. B. Wise, Phys. Rev. D **39**, 799 (1989); D. Scora and N. Isgur, Phys. Rev. D **52**, 2783 (1995).
[23] N. Barik, B. K. Dash, and P. C. Dash, Pramana J. Phys. **29**, 543 (1987); N. Barik, S. Kar, and P. C. Dash, Pramana J. Phys. **48**, 985 (1997); N. Barik, Sk. Naimuddin, S. Kar, and P. C. Dash, Phys. Rev. D **59**, 037301 (1998).
[24] N. Barik, P. C. Dash, and A. R. Panda, Phys. Rev. D **46**, 3856 (1992); N. Barik and P. C. Dash, *ibid.* **49**, 299 (1994); Mod. Phys. Lett. A **10**, 103 (1995); N. Barik, S. Kar, and P. C. Dash, Phys. Rev. D **57**, 405 (1998); N. Barik, Sk. Naimuddin, S. Kar, and P. C. Dash, Phys. Rev. D **63**, 014024 (2000); N. Barik, P. C. Dash, and A. R. Panda, Phys. Rev. D **47**, 1001 (1993); N. Barik and P. C. Dash, Phys. Rev. D **53**, 1366 (1996); N. Barik, S. K. Tripathy, S. Kar, and P. C. Dash, *ibid.* **56**, 4238 (1997); N. Barik, S. Kar, and P. C. Dash, Phys. Rev. D **63**, 114002 (2001); N. Barik, Sk. Naimuddin, and P. C. Dash, Int. J. Mod. Phys. A **24**, 2335 (2009).
[25] N. Barik, Sk. Naimuddin, P. C. Dash, and Susmita Kar, Phys. Rev. D **77**, 014038 (2008); **78**, 114030 (2008).
[26] F. J. Gilman and R. L. Singleton, Jr., Phys. Rev. D **41**, 142 (1990); J. G. Korner and G. A. Schuler, Mainz Report No. Mz-Th/88-14 (unpublished); Phys. Lett. B **226**, 185 (1989); H. Hangiwara, A. D. Martin, and M. F. Wade, *ibid.* **228**, 144 (1989).
[27] J. G. Korner and G. A. Schuler, Z. Phys. C **46**, 93 (1990).
[28] C. Amsler (Particle Data Group), Phys. Lett. B **667**, 1 (2008).
[29] M. Galdon and M. A. Sanchiz-lozano, Z. Phys. C **71**, 277 (1996).